Acta Crystallographica Section F
Structural Biology and Crystallization Communications
ISSN 1744-3091

The structure of the flexible arm of *Thermotoga maritima* tRNase Z differs from those of homologous enzymes

Ryohei Ishii,[a] Asako Minagawa,[b] Hiroaki Takaku,[b] Masamichi Takagi,[b] Masayuki Nashimoto[b] and Shigeyuki Yokoyama[a,c]*

[a]RIKEN Genomic Sciences Center, Tsurumi, Yokohama 230-0045, Japan, [b]Department of Applied Life Sciences, Niigata University of Pharmacy and Applied Life Sciences, Niigata 956-8603, Japan, and [c]Department of Biophysics and Biochemistry, Graduate School of Science, The University of Tokyo, Bunkyo-ku, Tokyo 113-0033, Japan

Correspondence e-mail: yokoyama@biochem.s.u-tokyo.ac.jp

Received 23 April 2007
Accepted 10 July 2007

PDB Reference: tRNase Z, 2e7y, r2e7ysf.

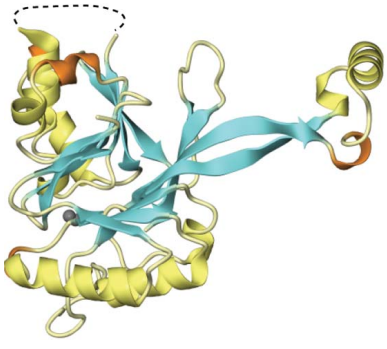

tRNA 3′-processing endoribonuclease (tRNase Z) is one of the enzymes involved in the 3′-end processing of precursor tRNAs and is a member of the metallo-β-lactamase superfamily. tRNase Z crystal structures have revealed that the enzyme forms a dimer and has a characteristic domain, named a flexible arm or an exosite, which protrudes from the metallo-β-lactamase core and is involved in tRNA binding. The refined structure of *Thermotoga maritima* tRNase Z has been determined at 1.97 Å resolution, revealing the structure of the flexible arm and the zinc-bound active site. The structure of the flexible arm of *T. maritima* tRNase Z is distinct from those of the *Bacillus subtilis* and *Escherichia coli* tRNase Zs. A comparison of the three tRNase Z structures revealed differences in the dimer orientation, which may be related to the unique cleavage-site specificity of *T. maritima* tRNase Z.

1. Introduction

Precursor tRNAs (pre-tRNAs) undergo several processing steps to generate mature functional tRNAs. Pre-tRNAs are transcribed as long forms with extra 5′ and 3′ sequences which must be removed (Deutscher, 1984, 1995; Morl & Marchfelder, 2001; Schurer *et al.*, 2001). The tRNA 3′-processing endoribonuclease, tRNase Z (EC 3.1.26.11; RNase Z or 3′-tRNase), is one of the ribonucleases involved in 3′-end processing and is conserved in almost all organisms (Levinger *et al.*, 1995; Nashimoto, 1995; Papadimitriou & Gross, 1996; Nashimoto *et al.*, 1999; Schierling *et al.*, 2002; Dubrovsky *et al.*, 2004; Minagawa *et al.*, 2004). In general, tRNase Z cleaves pre-tRNAs without the CCA sequence after the 'discriminator base' and the CCA sequence is enzymatically added downstream. In *Thermotoga maritima*, almost all pre-tRNAs have the CCA sequence and tRNase Z exceptionally cleaves precisely after the CCA sequence, not after the discriminator base (Minagawa *et al.*, 2004).

tRNase Z belongs to the metallo-β-lactamase superfamily, which fold into a four-layer $\alpha\beta/\beta\alpha$ sandwich fold and possess the characteristic 'histidine motif' for metal coordination (Tavtigian *et al.*, 2001; Aravind, 1999; Daiyasu *et al.*, 2001; Schiffer *et al.*, 2002). Furthermore, tRNase Z has an additional unique domain inserted in the metallo-β-lactamase domain, designated the 'flexible arm' or the 'exosite'. Biochemical and structural analyses revealed that the flexible arm is involved in tRNA binding (Spath *et al.*, 2005; Schilling, Spath *et al.*, 2005; Li de la Sierra-Gallay *et al.*, 2006).

Short and long forms of tRNase Z exist in nature. The short form of tRNase Z (tRNase Z^S/tRNase ZS/Elac1) consists of 280–360 amino-acid residues and is widely distributed among eukaryotes, bacteria and archaea. The long form of tRNase Z (tRNase Z^L/tRNase ZL/Elac2), which is found only in eukaryotes, consists of 750–930 amino-acid residues and is thought to have evolved from tRNase Z^S by gene duplication (Takaku *et al.*, 2004; Vogel *et al.*, 2005). In addition, tRNase Z^S is classified into two types according to the length of the flexible arm. The major type, named the zinc-dependent phosphodiesterase type (ZiPD-type), has a long flexible arm (~50 amino-acid residues) containing a proline-rich region. The minor type, named the TM-type, has a shorter flexible arm (~30 amino-acid residues) containing a basic residue-rich region and is found in *T. maritima* tRNase Z and *Arabidopsis thaliana* tRNase Z^S. In

contrast, tRNase Z^L has a longer flexible arm (~70 amino-acid residues) in the N-terminal half-domain but not in the C-terminal half-domain (Schilling, Spath *et al.*, 2005).

To date, three crystal structures of tRNase Z proteins, those from *T. maritima* (Ishii *et al.*, 2005), *Bacillus subtilis* (Li de la Sierra-Gallay *et al.*, 2005) and *Escherichia coli* (Kostelecky *et al.*, 2006), have been solved. Recently, the structure of the *B. subtilis* enzyme complexed with tRNA was also solved (Li de la Sierra-Gallay *et al.*, 2006). These structures revealed that tRNase Z has the canonical metallo-β-lactamase fold and forms a dimer. The active site is located near the dimer interface and the flexible arm, which clamps the tRNA, protrudes from the core into the solution.

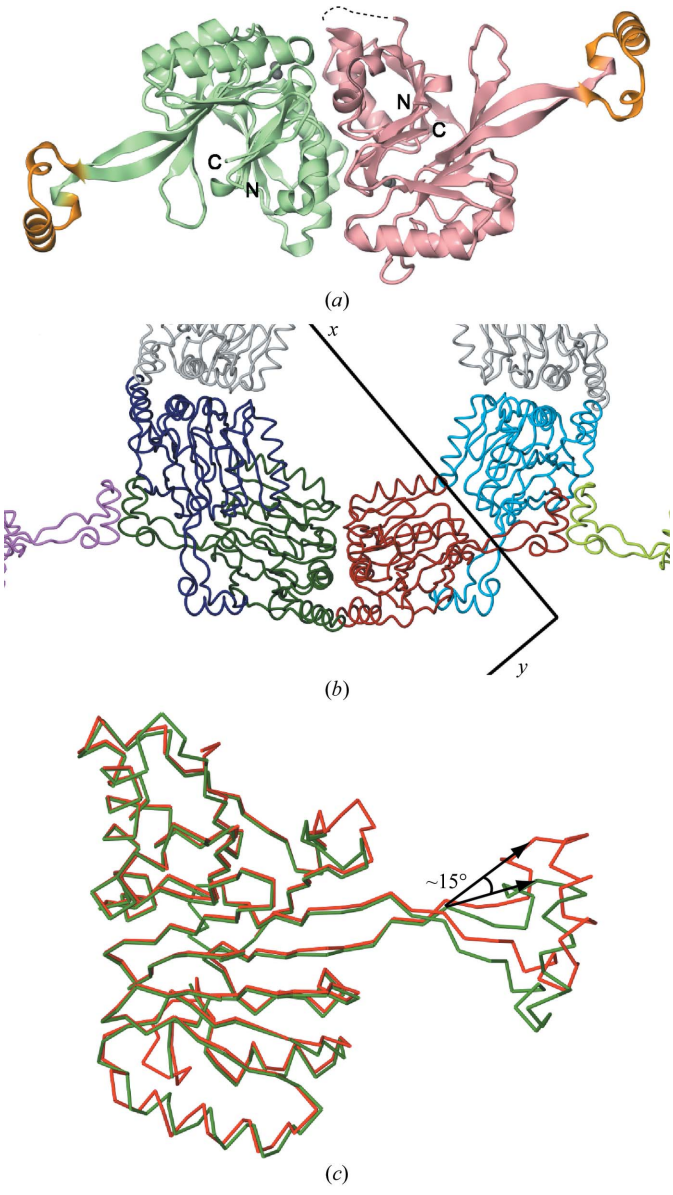

Figure 1
The *T. maritima* tRNase Z structure. (*a*) The *T. maritima* tRNase Z dimer structure. The two subunits are coloured green (subunit *A*) and pink (subunit *B*). Zn ions are depicted as grey spheres. The flexible arms (residues 153–176) are coloured orange. (*b*) Crystal packing of *T. maritima* tRNase Z. One subunit of the dimer is coloured green (subunit *A*) and the other is coloured red (subunit *B*). The symmetry-related molecules interacting with the dimer are coloured blue (symmetry operation $-x+1$, y, $-z+1/2$, subunit *A*), violet (symmetry operation $x+1/2$, $y+1/2$, z, subunit *B*), cyan (symmetry operation x, $-y$, $-z$, subunit *B*) and yellow-green (symmetry operation $x-1/2$, $y-1/2$, z, subunit *A*). (*c*) Superposition of the α-carbon chains of each subunit of *T. maritima* tRNase Z. The two subunits are coloured green (subunit *A*) and red (subunit *B*). The flexible arms were excluded from the superposition.

Table 1
Summary of data-collection and refinement statistics.

Values in parentheses are for the last shell.

Data collection	
X-ray source	PF NW12
Wavelength (Å)	0.9794
Space group	$C222_1$
Unit-cell parameters	
a (Å)	150.23
b (Å)	172.69
c (Å)	64.89
Resolution limits (Å)	40.0–1.97 (2.04–1.97)
Unique reflections	58453 (5449)
Redundancy	6.1 (4.5)
Completeness (%)	98.0 (92.4)
$I/\sigma(I)$	21.9 (2.4)
R_{sym}† (%)	12.0 (31.5)
Refinement	
Resolution limits (Å)	40.0–1.97 (2.09–1.97)
R_{work}‡	0.204 (0.280)
R_{free}‡	0.249 (0.324)
No. of reflections (working set)	55417 (8439)
No. of reflections (test set)	2950 (453)
No. of protein atoms	4462
No. of water atoms	325
No. of Zn atoms	4
Average B factor (Å^2)	
Protein atoms	50.61
Water atoms	52.74
Zn atoms	57.13
R.m.s.d. bond lengths (Å)	0.0091
R.m.s.d. bond angles (°)	1.50
Ramachandran plot (%)	
Most favoured	91.2
Additionally allowed	7.3
Generously allowed	1.0
Disallowed	0.4 [Asp25]

† $R_{sym} = \sum|I_{hkl} - \langle I_{hkl}\rangle|/\sum I_{hkl}$, where $\langle I_{hkl}\rangle$ is the mean value of I_{hkl}. ‡ $R_{work} = \sum|F_o - F_c|/\sum F_o$, where F_o is the observed structure-factor amplitude and F_c is the structure factor calculated from the model. R_{free} is calculated in the same manner as R_{work} using the test set of reflections (5% of the total reflections).

We previously solved the crystal structure of *T. maritima* tRNase Z at 2.6 Å resolution (Ishii *et al.*, 2005). However, the structure of the flexible arm, which is important for tRNA binding, could not be determined and the state of the metal-coordinated active site was not clear. Here, we report the crystal structure of *T. maritima* tRNase Z at a higher resolution (1.97 Å) determined in space group $C222_1$, which is the first to reveal the structures of the *T. maritima* tRNase Z flexible arm and the zinc-bound active site. A comparison of the structure of *T. maritima* tRNase Z with those of homologous enzymes provides insights into the differences between these enzymes.

2. Materials and methods

2.1. Protein purification and crystallization

T. maritima tRNase Z protein was expressed and purified using previously described procedures (Ishii *et al.*, 2005). Prior to crystallization, the protein fraction was dialyzed against 20 m*M* HEPES buffer pH 7.0 containing 400 m*M* NaCl and 10 m*M* β-mercaptoethanol and was concentrated to approximately 2.0 mg ml^{-1} using a Vivaspin2 filter (Vivascience).

Crystallization was accomplished using the hanging-drop vapour-diffusion method at 293 K. The drops were formed by mixing 1 µl protein solution with 1 µl reservoir solution (0.1 *M* Tris–HCl buffer pH 8.5 containing 10% PEG 4000 and 0.5 *M* Li_2SO_4). Plate-shaped crystals with dimensions of 300 × 300 × 100 µm were obtained within a week.

2.2. Data collection, structure determination and refinement

The crystals were transferred into a cryoprotectant solution consisting of mother liquor plus 35%(*v*/*v*) 1,2-propanediol and were flash-cooled in liquid nitrogen. The data set for the crystal was collected at 100 K on a Quantum-210 CCD detector (Area Detector Systems Corp.) at beamline NW12, Photon Factory, Tsukuba, Japan. Data processing and scaling were performed with the *HKL*-2000 program suite (Otwinowski & Minor, 1997).

The high-resolution structure was solved by molecular replacement using the program *MOLREP* (Vagin & Teplyakov, 1997) and the previously determined *T. maritima* tRNase Z dimer (PDB code 1ww1) as a search model. All refinements were performed with *CNS* (Brünger *et al.*, 1998). The first round of refinement consisted of rigid-body refinement, was followed by energy minimization, refinement of individual *B* factors and simulated annealing. After simulated annealing, a clearly interpretable electron-density map of the flexible arm was calculated. The atomic model was manually built using *O* (Jones *et al.*, 1991) and was refined using the same *CNS* procedures as used in the first round of refinement. Some loop regions (amino-acid residues 213–220 of molecule *A* and 67–71 and 133–138 of molecule *B*) were not visible and were excluded from the final model, which had *R* and $R_{\rm free}$ factors of 20.4% and 24.9%, respectively. The model shows good geometry as evaluated by *PROCHECK* (Laskowski *et al.*, 1993), with all residues in the allowed regions of the Ramachandran plot except for two residues (Asp25 in each subunit),. The data-collection and refinement statistics are shown in Table 1.

3. Results and discussion

3.1. Overall structure

Using the molecular-replacement method, the high-resolution structure of *T. maritima* tRNase Z was solved at 1.97 Å resolution in the *C*-centred orthorhombic form. In the crystal, the asymmetric unit contains two molecules (*A* and *B*), which form a dimer (Fig. 1*a*). The core structure of the *T. maritima* tRNase Z dimer is essentially similar to the previous structure (r.m.s.d. of 1.2 Å for 464 C^{α} atoms), which was determined in space group $P2_12_12$. Unlike the previous structure, the flexible arms are stabilized owing to the crystal contacts between the symmetry-related molecules (Figs. 1*a* and 1*b*).

3.2. Structure of the flexible arm of *T. maritima* tRNase Z

The flexible arm of *T. maritima* tRNase Z (amino-acid residues 153–176) consists of two α-helices (Fα1 and Fα2), one of which is very short and the other long, and a 3_{10}-helix (Fη1) (Figs. 1*a* and 2*a*). The long α-helix (Fα2) is connected by the short helices to the β-strands protruding from the core. In contrast, the flexible arms of the *B. subtilis* and *E. coli* tRNase Zs consist of two α-helices, two β-strands and one 3_{10}-helix (Fig. 2*a*; Li de la Sierra-Gallay *et al.*, 2005; Kostelecky *et al.*, 2006). Therefore, the topology as well as the length of the flexible arm of *T. maritima* tRNase Z differs from those of the *B. subtilis* and *E. coli* tRNase Zs (Fig. 2*b*).

Crystallographic contacts could stabilize the structure of the flexible arm. In brief, the outer face of the flexible arm contacts that of the other protomer related by crystallographic symmetry. The inner face of the flexible arm mainly contacts β7 and the following loop in the corresponding protomer related by crystallographic symmetry (Fig. 1*b*). The mode of contact differs slightly in molecules *A* and *B*. As a result, the angles between the metallo-β-lactamase core and the flexible arm differ by about 15° (Fig. 1*c*), indicating the mobility of the flexible arms of *T. maritima* tRNase Z in solution.

3.3. Active site

The active site of tRNase Z is expected to contain two metal ions coordinated by five histidine residues and one aspartate residue, in a manner similar to those of other metallo-β-lactamase superfamily members (Vogel *et al.*, 2002). However, the structures of the active sites of the three enzymes differ in terms of the metal-binding mode. In the previous *T. maritima* tRNase Z structure, only one unidentified metal ion was bound in both active sites (Ishii *et al.*, 2005). In contrast, in the *B. subtilis* tRNase Z structure two zinc ions were present at the

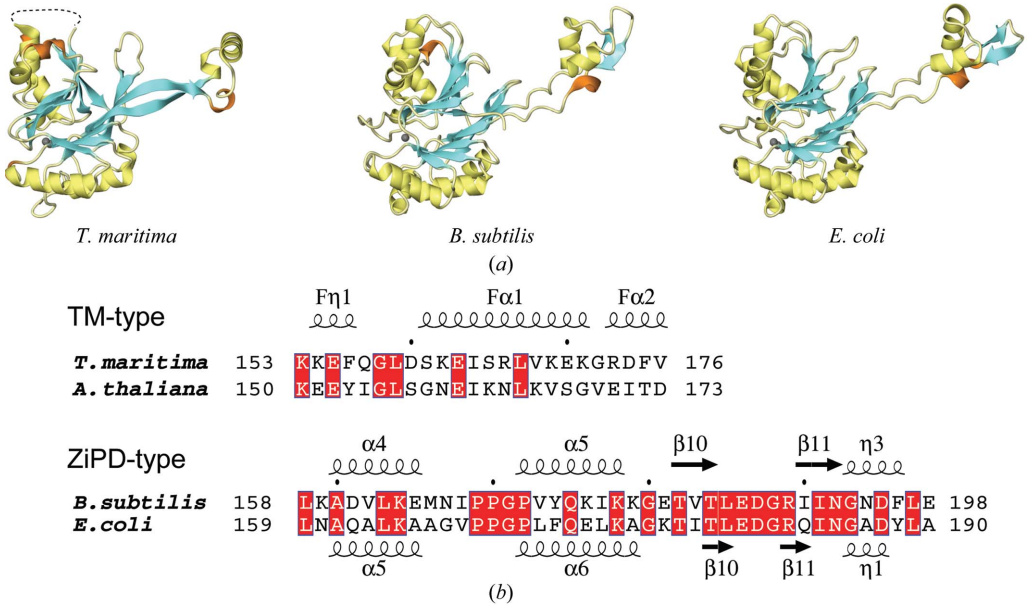

Figure 2
Comparison of the structure of the *T. maritima* tRNase Z monomer with those of the *B. subtilis* and *E. coli* tRNase Zs. (*a*) Ribbon diagram displaying the overall monomeric structures of the three tRNase Zs. The α-helices, β-strands and 3_{10}-helices are coloured yellow, cyan and orange, respectively. Zn ions are depicted as grey spheres. The multiple three-dimensional structure alignment of the core structures was carried out using the Secondary Structure Matching server (Krissinel & Henrick, 2004). (*b*) Sequence alignment of the flexible arms of tRNase Zs. α-Helix, β-strand and 3_{10}-helix secondary structures are denoted by the Greek characters α, β and η, respectively. The red boxes show the residues conserved in each type of tRNase Z.

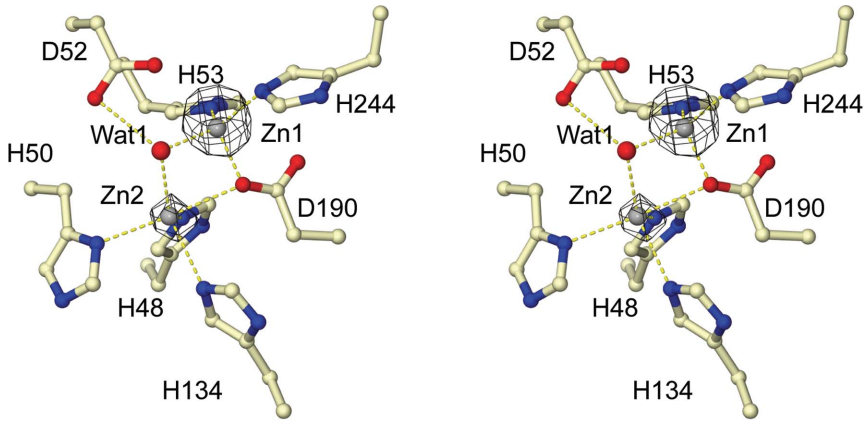

Figure 3
Stereoview of the active site of *T. maritima* tRNase Z. The side chains interacting with the zinc ions in subunit *A* are depicted as ball-and-stick models. The zinc ions and the water are depicted as grey and red spheres, respectively. The anomalous difference map (contoured at the 3σ level) calculated from the data collected at the zinc peak wavelength (1.279 Å) is also superimposed (black).

active site of subunit *A* and no metal ion was associated with subunit *B*, indicating flexibility in this region (Li de la Sierra-Gallay *et al.*, 2005). In the *E. coli* tRNase Z structure, in which the crystallographic symmetry-related molecules form the dimer, two zinc ions were bound within the active site, probably owing to the presence of zinc ions in the crystallization conditions (Kostelecky *et al.*, 2006).

In the density map of the present *T. maritima* tRNase Z crystal, there were two strong electron densities (>3σ) in the active site in both subunits. An X-ray absorption fine-structure spectrum (see supplementary material[1]) and an anomalous difference map, measured at the Zn peak wavelength (1.2791 Å), confirmed that the strong electron densities are derived from zinc ions (Fig. 3). The conformations of the active sites in both subunits are essentially the same, with an r.m.s.d. of 0.15 Å for all metal ligand atoms, except for His134 in molecule *B*, which is disordered. One zinc ion (Zn1), which was also bound in the previous structure, is coordinated by two histidine residues (His53 and His244), one aspartate residue (Asp190) and a bridging water molecule (Wat1). Wat1 also makes hydrogen bonds with the side chain of Asp52. The other zinc ion (Zn2) is coordinated by three histidine residues (His48, His50 and His134), one aspartate residue (Asp190) and one water molecule (Wat1) (Fig. 3). Therefore, Zn1 is coordinated with tetrahedral geometry and Zn2 is coordinated with trigonal bipyramidal geometry. The architecture of the active site resembles that observed in the *B. subtilis* and *E. coli* tRNase Z structures (Li de la Sierra-Gallay *et al.*, 2005; Kostelecky *et al.*, 2006).

Although the anomalous difference map clearly shows the existence of two Zn ions in the active site, their binding affinities seem to differ. There is a stronger peak around Zn1 than around Zn2 in the anomalous difference map (Fig. 3). The refined *B* factors are about 45 and 70 Å^2 for Zn1 and Zn2, respectively. An occupancy refinement using *CNS* indicated that the occupancies of Zn1 and Zn2 are about 1.0 and 0.5, respectively, on the assumption that they have the same *B* factor (45 Å^2). In addition, the average distance between Zn1 and the coordinated ligands is 2.1 Å, which is a typical distance between a zinc ion and a ligand (Harding, 2001). In contrast, the average distance between Zn2 and the coordinated ligands is 2.5 Å, which is slightly longer than the typical distance. Since we did not add any zinc ions during purification and crystallization, the bound zinc ions were copurified with the protein. Hence, these findings suggest that Zn1 binds more tightly than Zn2 and that Zn2 easily dissociates from the active site. It has been reported that the metal-binding affinities of *E. coli* tRNase Z also differ (Schilling, Vogel *et al.*, 2005). A high zinc ion concentration abolishes the *T. maritima* tRNase Z activity (Minagawa *et al.*, 2006), implying that dissociation of the zinc ion(s) from the active site might be indispensable for its activity.

3.4. The orientation of the two monomers differs between the *T. maritima* tRNase Z and the *B. subtilis*/*E. coli* tRNase Zs

Interestingly, a comparison of the dimeric structures of the *T. maritima* and *B. subtilis* tRNase Zs revealed a significant difference in the orientations of the dimers. When one subunit core of the *T. maritima* tRNase Z dimer was superimposed on that of *B. subtilis* tRNase Z, a rotation of about 23° and a slight translation (~1 Å) along a screw axis was required to superimpose the other subunit core of *T. maritima* tRNase Z on that of *B. subtilis* tRNase Z (Fig. 4*a*). The angle between the screw axis and the pseudo-twofold axis of *T. maritima* tRNase Z is about 80°. As a result, the angle between the two subunits of *T. maritima* tRNase Z is smaller than that of *B. subtilis* tRNase Z (Fig. 4*a*).

One of the possible reasons for the smaller angle in *T. maritima* tRNase Z is that the length of the loop connecting β1 and β2 differs between *T. maritima* tRNase Z and the other tRNase Zs. In *T. maritima* tRNase Z the loop is composed of three amino-acid residues, whereas the loops in the *B. subtilis*/*E. coli* tRNase Zs are composed of 14 amino-acid residues (Figs. 4*b* and 4*c*). The loop is located at the dimer interface and interacts with α1 of the other subunit. Thus, if the loop is longer then a wider angle is required to avoid steric hindrance. In addition, the loop is adjacent to the entrance of the active site, implying that this region could interact with the pre-tRNA and be involved in cleavage-site selection.

4. Conclusions

The high-resolution structure of *T. maritima* tRNase Z revealed the structure of the flexible arm involved in pre-tRNA binding. This structure also validated the existence of two zinc ions at the active site. A comparison of the structures of the *T. maritima* and *B. subtilis* tRNase Zs suggested that a difference in the orientations of the dimers is responsible for the substrate specificity. Since *T. maritima* tRNase Z cleaves the pre-tRNA after the CCA sequence, while *B. subtilis* tRNase Z cleaves the pre-tRNA without the CCA

[1] Supplementary material has been deposited in the IUCr electronic archive (Reference: SW5017).

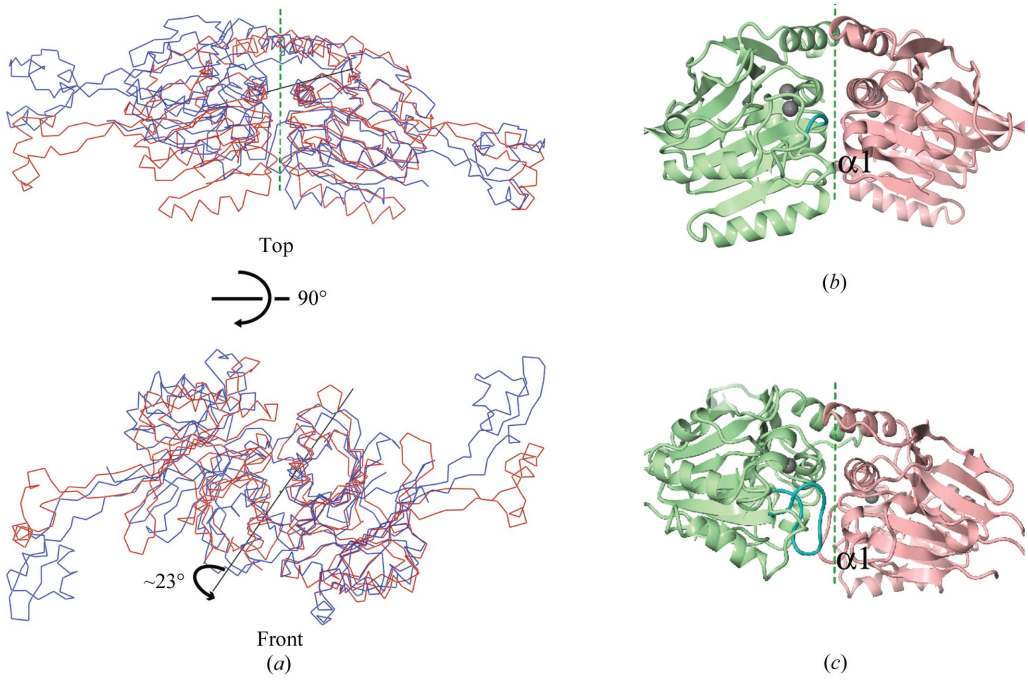

Figure 4
Comparison of the structure of the *T. maritima* tRNase Z dimer with that of the *B. subtilis* tRNase Z dimer complexed with tRNA. (*a*) Superposition of the *T. maritima* tRNase Z dimer (red) and the *B. subtilis* tRNase Z dimer (blue). The right subunits of the dimers were superimposed using the Secondary Structure Matching server (Krissinel & Henrick, 2004). The black line indicates the screw axis to superimpose one protomer of *T. maritima* tRNase Z onto that of *B. subtilis* tRNase Z and the green dashed line indicates the pseudo-twofold axis of the *T. maritima* tRNase Z dimer. The pseudo-twofold axis is parallel (top panel) and perpendicular (bottom panel) to the paper. (*b*) The dimer interface of *T. maritima* tRNase Z and (*c*) that of *B. subtilis* tRNase Z. The two subunits are coloured green and pink, respectively. Zn ions are depicted as grey spheres. The loop connecting β1 and β2 is coloured cyan. The orientation of tRNase Z is the same as in the top panel of (*a*).

sequence after the discriminator base, there must be a region that recognizes the CCA sequence in tRNase Z. To elucidate how tRNase Z recognizes the pre-tRNA and the CCA sequence, the high-resolution structure of the enzyme complexed with the pre-tRNA must be solved.

We thank the staff of beamlines NW12 and BL-5A at the Photon Factory, Tsukuba, Japan as well as the staff of beamline BL41XU at SPring-8, Harima, Japan for assistance during data collection. This work was supported in part by the RIKEN Structural Genomics/Proteomics Initiative (RSGI) in the National Project on Protein Structural and Functional Analyses of the Ministry of Education, Culture, Sports, Science and Technology (MEXT) of Japan and by Grants-in-Aid for Scientific Research on Priority Areas from MEXT.

References

Aravind, L. (1999). *In Silico Biol.* **1**, 69–91.
Brünger, A. T., Adams, P. D., Clore, G. M., DeLano, W. L., Gros, P., Grosse-Kunstleve, R. W., Jiang, J.-S., Kuszewski, J., Nilges, M., Pannu, N. S., Read, R. J., Rice, L. M., Simonson, T. & Warren, G. L. (1998). *Acta Cryst.* D**54**, 905–921.
Daiyasu, H., Osaka, K., Ishino, Y. & Toh, H. (2001). *FEBS Lett.* **503**, 1–6.
Deutscher, M. P. (1984). *CRC Crit. Rev. Biochem.* **17**, 45–71.
Deutscher, M. P. (1995). *tRNA: Structure, Biosynthesis and Function*, edited by D. Soll & U. L. RajBhandary, pp. 51–65. Washington, DC: ASM Press.
Dubrovsky, E. B., Dubrovskaya, V. A., Levinger, L., Schiffer, S. & Marchfelder, A. (2004). *Nucleic Acids Res.* **32**, 255–262.
Harding, M. M. (2001). *Acta Cryst.* D**57**, 401–411.
Ishii, R., Minagawa, A., Takaku, H., Takagi, M., Nashimoto, M. & Yokoyama, S. (2005). *J. Biol. Chem.* **280**, 14138–14144.
Jones, T. A., Zou, J.-Y., Cowan, S. W. & Kjeldgaard, M. (1991). *Acta Cryst.* A**47**, 110–119.
Kostelecky, B., Pohl, E., Vogel, A., Schilling, O. & Meyer-Klaucke, W. (2006). *J. Bacteriol.* **188**, 1607–1614.
Krissinel, E. & Henrick, K. (2004). *Acta Cryst.* D**60**, 2256–2268.
Laskowski, R. A., Moss, D. S. & Thornton, J. M. (1993). *J. Mol. Biol.* **231**, 1049–1067.
Levinger, L., Vasisht, V., Greene, V., Bourne, R., Birk, A. & Kolla, S. (1995). *J. Biol. Chem.* **270**, 18903–18909.
Li de la Sierra-Gallay, I., Mathy, N., Pellegrini, O. & Condon, C. (2006). *Nature Struct. Mol. Biol.* **13**, 376–377.
Li de la Sierra-Gallay, I., Pellegrini, O. & Condon, C. (2005). *Nature (London)*, **433**, 657–661.
Minagawa, A., Takaku, H., Ishii, R., Takagi, M., Yokoyama, S. & Nashimoto, M. (2006). *Nucleic Acids Res.* **34**, 3811–3818.
Minagawa, A., Takaku, H., Takagi, M. & Nashimoto, M. (2004). *J. Biol. Chem.* **279**, 15688–15697.
Morl, M. & Marchfelder, A. (2001). *EMBO Rep.* **2**, 17–20.
Nashimoto, M. (1995). *Nucleic Acids Res.* **23**, 3642–3647.
Nashimoto, M., Tamura, M. & Kaspar, R. L. (1999). *J. Mol. Biol.* **287**, 727–740.
Otwinowski, Z. & Minor, W. (1997). *Methods Enzymol.* **276**, 307–326.
Papadimitriou, A. & Gross, H. J. (1996). *Eur. J. Biochem.* **242**, 747–759.
Schierling, K., Rosch, S., Rupprecht, R., Schiffer, S. & Marchfelder, A. (2002). *J. Mol. Biol.* **316**, 895–902.
Schiffer, S., Rosch, S. & Marchfelder, A. (2002). *EMBO J.* **21**, 2769–2777.
Schilling, O., Spath, B., Kostelecky, B., Marchfelder, A., Meyer-Klaucke, W. & Vogel, A. (2005). *J. Biol. Chem.* **280**, 17857–17862.
Schilling, O., Vogel, A., Kostelecky, B., Natal da Luz, H., Spemann, D., Spath, B., Marchfelder, A., Troger, W. & Meyer-Klaucke, W. (2005). *Biochem. J.* **385**, 145–153.
Schurer, H., Schiffer, S., Marchfelder, A. & Morl, M. (2001). *Biol. Chem.* **382**, 1147–1156.
Spath, B., Kirchner, S., Vogel, A., Schubert, S., Meinlschmidt, P., Aymanns, S., Nezzar, J. & Marchfelder, A. (2005). *J. Biol. Chem.* **280**, 35440–35447.
Takaku, H., Minagawa, A., Takagi, M. & Nashimoto, M. (2004). *Nucleic Acids Res.* **32**, 4429–4438.
Tavtigian, S. V. *et al.* (2001). *Nature Genet.* **27**, 172–180.
Vagin, A. & Teplyakov, A. (1997). *J. Appl. Cryst.* **30**, 1022–1025.
Vogel, A., Schilling, O., Niecke, M., Bettmer, J. & Meyer-Klaucke, W. (2002). *J. Biol. Chem.* **277**, 29078–29085.
Vogel, A., Schilling, O., Spath, B. & Marchfelder, A. (2005). *Biol. Chem.* **386**, 1253–1264.